In-situ Crack Propagation Observation of a Particle Reinforced Polymer Composite Using the Double Cleavage Drilled Compression Specimens

Yeon Soo Lee
Center for Joint Disease, Chonnam National University Hwasun Hospital, Ilsimli 160, Hwasun Eup, Hwasun Gun, Jeonlanamdo, Korea
Young Ki Yoon
Defense Acquisition Program Administration, Yongsan-dong 2-ga 2-15, Yongsan-gu, Seoul 140-833, Korea
Bo Young Jeong, Hi Seak Yoon*
School of Mechanical Systems Engineering, Chonnam National Univeristy, YongBong-Dong 300, Buk-gu, GwangJu 500-757, Korea

In this study, we investigate the feasibility of in-situ crack propagation by using a double cleavage drilled compression (DCDC) specimen showing a slow crack velocity down to 0.03 mm/s under 0.01 mm/s of displacement control. Finite element analysis predicted that the DCDC specimens would show at least 4.3 fold delayed crack initiation time than conventional tensile fracture specimens under a constant loading speed. Using DCDC specimens, we were able to observe the in-situ crack propagation process in a particle reinforced transparent polymer composite. Our results confirmed that the DCDC specimen would be a good candidate for the in-situ observation of the behavior of particle reinforced composites with slow crack velocity, such as the self-healing process of micro-particle reinforced composites.

Key Words : Double Cleavage Drilled Compression (DCDC) Specimen, Crack Propagation, Stress Intensity Factor, In-Situ Observation, Self-Healing

1. Introduction

Delayed failure in composites containing reinforcing materials or voids is interesting due to the possibility of observing crack propagation and crack growth behavior (Lee and Tomozawa, 1999; Yoshida et al., 2001). A crack front with slow matrix crack growth can be directly observed in a double-cleavage-drilled compression (DCDC) specimen (He et al., 1995; Janssen, 1974; 1980; Jenne et al., 2003; Kagawa and Goto, 1998; Lee and Tomozawa, 1999; Michalske et al., 1993; Yoshida et al., 2001).

The double cleavage drilled compression (DCDC) specimen was developed by Janssen to obtain a specimen with a crack length independent K_I (Janssen, 1974; Janssen, 1980). DCDC specimens have many advantages including resistance to compressive loading, mid-plane crack stability, and auto-precracking (Janssen, 1980). DCDC specimens were used to initiate slow crack growth (Kagawa and Goto, 1998; Lee and Tomozawa, 1999) and to directly observe crack front shape in-situ (Kagawa and Goto, 1998). With a double cantilever cleavage (DCC) geometry, stress intensity increases as the crack length increases under a constant applied load (Crichton and Tomozawa,

* Corresponding Author,
E-mail : hsyoon@jnu.ac.kr
TEL : +82-62-530-1671; **FAX** : +82-62-530-1689
School of Mechanical Systems Engineering, Chonnam National Univeristy, YongBong-Dong 300, Buk-gu, GwangJu 500-757, Korea. (Manuscript **Received** July 2, 2005; **Revised** January 12, 2006)

1999), and thus crack velocity accelerates throughout the measurement (Weiderhorn, 1967). Unlike the DCC specimens, the DCDC geometry features a stress intensity that decreases with crack growth under a constant applied load. Thus, DCDC geometry is more stable since crack propagation is retarded (Crichton and Tomozawa, 1999). And Janssen's double cleavage drilled compression (DCDC) specimen was recommended by Yoshida et al.(2001) as a good specimen for observing crack propagation in a very brittle glass.

This study attempts to observe crack growth in a particle-reinforced composite by using the DCDC specimen. For direct observation of crack propagation, we adopted a transparent epoxy as the matrix of the DCDC specimen containing ceramic particles. We clarify the terms related to the double cleavage drilled (DCD) specimens as follows. The double cleavage drilled compression (DCDC) specimen was defined as the DCD specimen whose crack propagation is derived by externally applied compression (Janssen, 1974), while the double cleavage drilled tension (DCDT) specimen as the DCD specimen whose crack propagation is derived by externally applied tension. Based on the results of this study, we discussed the possibility of using the DCDC specimen to observe the self-healing mechanisms in situ, such as, the autonomic polymerization process of self-healing materials.

2. Materials and Methods

2.1 Experimental specimens

Commercially available CZC particles made of ZrO_2 (Cenotec Co., Masan, Korea) were embedded in a commercially available transparent epoxy MS-200 (Nippon Steel Chemical Co., Japan). The material properties of MS-200 epoxy and CZC (ZrO_2) particles are listed in Table 1. The diameter of the CZC particle was 1 mm. Transparent MS-200 powder and 0.15% volume fraction of CZC particles were mixed into a customized mold. Then the mixture was hot- pressed to shape as a DCDC specimen for 10 minutes at pressing pressure of 10 MPa and temperature of 463 K. The DCDC specimen was a 40 mm×40 mm×10 mm plate with a 8 mm hole and two full-thickness grooves representing a pre-crack of length, width, and end diameter of 2 mm (i.e. a_0=2 mm), 0.5 mm, and 0.5 mm, respectively (Fig. 1). All the specimen surfaces including the inside of the center hole were mechanically ground and polished to remove all visible scratches.

Table 1 Mechanical properties of the used material

	CZC (ZrO_2)	MS-200
Elastic Modulus (GPa)	110	2
Tensile Strength (MPa)	343	588

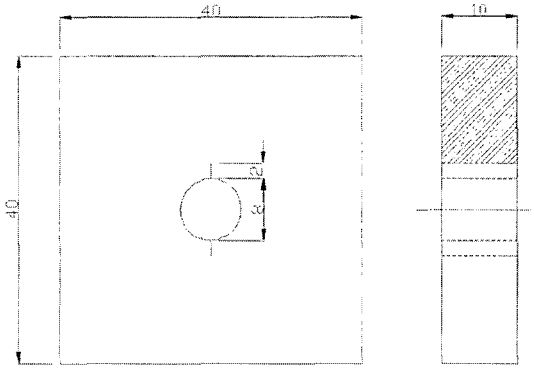

Fig. 1 The dimensions of the DCDC specimen. The DCD specimen was a 40×40×10 mm^3 plate which has a hole of 8 mm diameter and two full-thickness groove of 2 mm length

2.2 Finite element analysis using a DCDC specimen model

The effect of DCDC testing on crack propagation was evaluated and compared with that of DCDT testing by finite element analysis. By applying different loading conditions to a double cleavage drilled (DCD) specimen model, both the double cleavage drilled compression (DCDC) mode and the double cleavage drilled tension (DCDT) mode were analyzed. Because of structural symmetry, only a quarter of the isotropic DCD plate with dimensions of was modeled to include a hole of 8 mm diameter but not the groove (Fig. 3). Because the main purpose of the finite element analysis (FEA) was to evaluate the crack propagation rate of DCDC specimens versus DCDT specimens, the particles and the

grooves were not modeled in the FEA model. Using ABAQUS v6.3, a commercial finite element software analysis package, the model was analyzed in the linear elastic mode.

A uniform load distribution was applied to the loading surface (Fig. 3). The loading speed was $\dot{\sigma}_{app}=1\ \mathrm{N/m^2}$ and the final load was reached up to $70\ \mathrm{N/m^2}$. Corning Macor® Machineable Glass (Corning Inc., NY, USA) was temporarily selected only for the purpose of computational analysis. Young's modulus and Poisson's ratio of Corning Macor® Machineable Glass are 66.9 GPa and 0.29, respectively. The full-thickness crack initiation time was defined as the time required for the stress intensity factors of all crack tip nodes to become higher than the fracture toughness of the Corning Macor® Machineable Glass ($K_{IC}=1.53\ \mathrm{MPa\cdot m^{1/2}}$).

2.3 Fracture tests of DCDC specimen

The compression test machine used was an Instron 8872. The loading cross-head speed was 0.01 mm/s by displacement control. A digital CCD video microscope camera was used to observe crack propagation in the direction parallel to the crack plane. Images from the CCD camera were acquired with a magnification of ×100 and saved to a personal IBM computer (Fig. 2). The crack propagation length, $a-a_0$, was defined as the length from the location of the groove end to the location of the crack front. The locations of groove end and crack front were measured at the middle of the specimen thickness because the crack at the middle of the specimen thickness had highest stress intensity along the thickness and also the crack grew faster in the middle of thickness than on the surface (Kagawa and Goto,

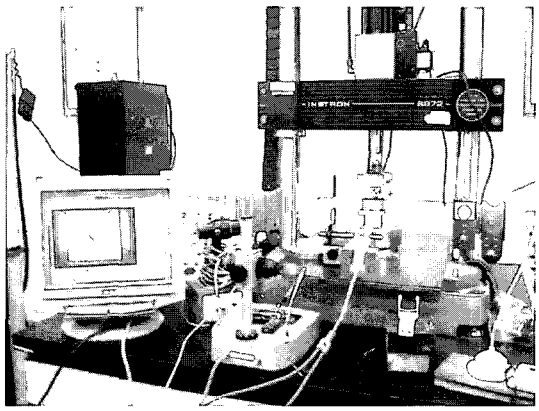

Fig. 2 Experimental test setup. An in situ direct observation system of the crack propagation was set up for the test of DCDC specimens

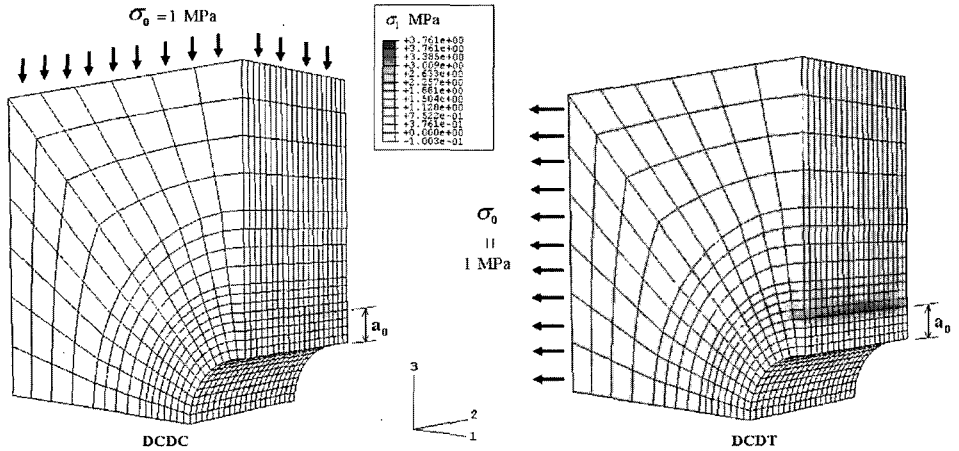

Fig. 3 FEA model and expected stress distributions of double-cleavage drilled (DCD) specimens. A DCD specimen subjected to compression (DCDC) and a DCD specimen to tension (DCDT) were analyzed by finite element method under $\sigma_0=1$ MPa when $a_0=2$ mm. The crack tip opening stress (σ_1) along the crack tip line showed a convex curve which was the lowest in the edge and the highest at the center along the thickness direction (i.e. along the direction 2)

1998). The applied plane stress intensity factor, K^{app}, of the DCDC specimen was calculated by using the experimental formula obtained by Kagwa and Goto (1998) as

$$K^{app}=\sigma_{app}a^{0.5}\cdot F\left(\frac{a}{r}\right) \quad (1)$$

where σ_{app} is the applied stress, a and r are the crack length and the radius of the hole at the center of the DCDC specimen, respectively. $F(a/r)$ is the shape factor available in $a/r=0.5\sim3$ (Kagawa and Goto, 1998).

3. Results

3.1 Initial crack initiation time of the DCDC specimen by FEA

The crack tip opening stress, σ_1, on the crack tip line gave a convex curve, whose lowest point was at the edge and the highest at the center in the thickness direction (i.e., along the direction 2 in Fig. 3). The stress intensity factor (K_I), evaluated through the finite element analysis, was normalized by $\sigma_{app}\sqrt{\pi a_0}$ to use in comparisons without considering the effect of externally applied stress. The applied uniform load, σ_{app}, was 1 MPa. At the crack tip, the normalized stress intensity of the DCDC specimen, $K_I/(\sigma_{app}\sqrt{\pi a_0})$, was much lower than that of DCDT specimen (Fig. 4). The stress intensity ratio of DCDC to DCDT ($K_{I(DCDC)}/K_{I(DCDT)}$) was 0.15 at the edge and 0.23 at the center (Fig. 4). Under the same loading rate, the normalized stress intensity ($K_I/\sigma_{app}\sqrt{\pi a_0}$) of the DCDT specimen showed much higher values than that of the DCDC specimen (Fig. 5). Considering the fracture toughness of the Corning Macor® Machineable Glass, the full-thickness crack initiation was predicted to occur at 9 seconds and at 39 seconds under $\dot{\sigma}_{app}=1$ N/mm^2/s for the DCDT and DCDC specimens, respectively (Fig. 5). Hence, it can be expected that the DCDC specimens would show at least 4.3 fold delayed crack initiation time than con-

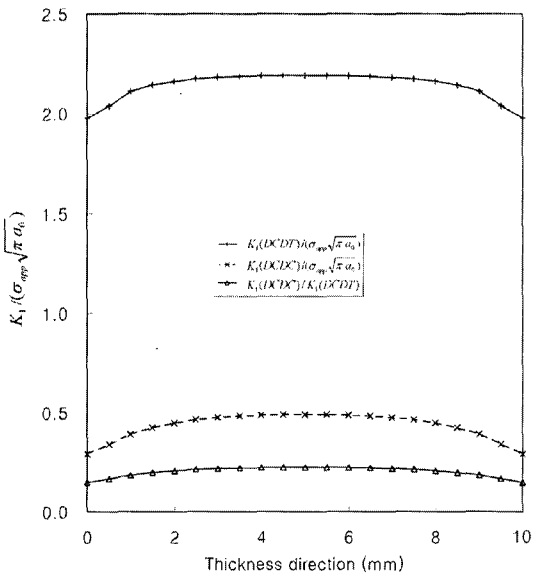

Fig. 4 Normalized expected stress intensity factors of DCD specimens. Stress intensity factors of DCDT and DCDT specimens were normalized by the $\sigma_{app}\sqrt{\pi a_0}$ (with $a_0=2$ mm). The stress intensity ratio of DCDC to DCDT ($K_{I(DCDC)}/K_{I(DCDT)}$) was 0.15 at the edge and 0.22 at the thickness center

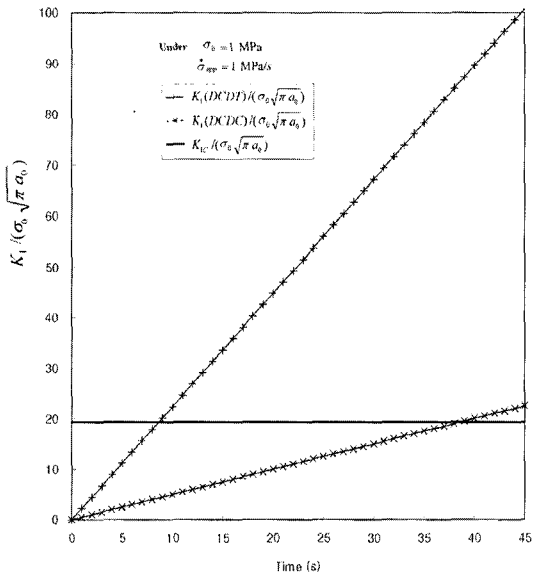

Fig. 5 Normalized expected stress intensity of the DCDC and DCDT specimens under $\dot{\sigma}_{app}=1$ N/mm^2/s. The stress intensity factor (K_I) and the fracture toughness (K_{IC}) was normalized by $\sigma_0\sqrt{\pi a_0}$ (with $\sigma_0=1$ MPa, $a_0=2$ mm). The full-thickness crack initiation occurred at 39 s for the DCDC specimen and 9 s for DCDT specimen

ventional tensile fracture specimens under a constant loading speed.

2.2 Fracture test results of the DCDC specimen

Under 0.01 mm/s of displacement control, the applied force and the crack length were recorded according to the time. Then, the applied nominal stress according to the crack propagation was evaluated, as shown in Fig. 6, where specimen 1 denotes a pure epoxy and specimen 2 denotes a 3% CZC/epoxy composite. The applied stress of the composite is bigger that that of pure epoxy, and hence, the composite specimen requires a larger applied stress for crack growth than the pure epoxy specimen does. However, the applied stress of the pure epoxy becomes the same as that of the composite as the crack grows further. It can be concluded that the fracture resistance after a critical crack growth is only dependent on the crack tip geometry.

From Fig. 6, average crack propagation speed ($\dot{a}$) can be calculated at the first maximum point where the applied stress is 48.8 MPa. At that point, the crack length was 3.9 mm and the elapsed time was approximately 125 s in the case of CZC/epoxy composite. Therefore the average crack propagation speed ($\dot{a}$) of CZC/epoxy composite was calculated as 0.031 mm/s. By using the same method, the average crack propagation speed of the pure epoxy specimen was calculated as 0.039 mm/s. Hence, it can be shown that CZC/epoxy composite slowed slower crack propagation.

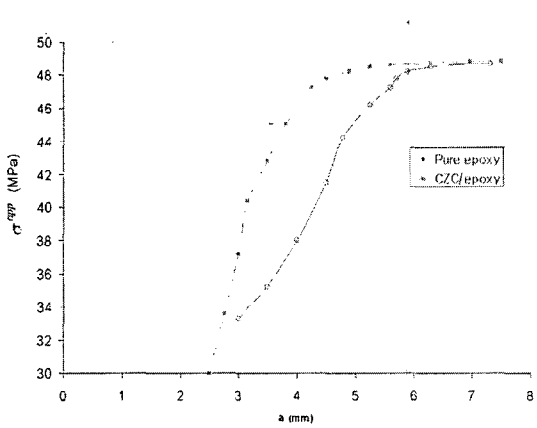

Fig. 6 Applied nominal stress according to crack propagation length. CZC particle reinforced composite DCDC specimens were tested. The crack propagation speed ($\dot{a}$) was calculated on the graph at the earliest maximum point of the applied stress of 48.8 MPa. The average crack propagation speed ($\dot{a}$) until it gets 3.9 mm is calculated as 0.031 mm/s in the case of the CZC/epoxy composite and 0.039 mm/s in the case of pure epoxy

The applied stress intensity factor was also evaluated by Eq. (1) and plotted against to the crack length over the radius of the hole (a/r) as shown in Fig. 7. Under the displacement control of 0.01 mm/s, the stress intensity factor of CZC/epoxy composite was bigger than that of pure epoxy. Therefore, it can be concluded that the fracture toughness of the CZC/epoxy composite, compared to that of pure epoxy, was reduced by the hard particles.

Figure 8 shows the effect of the hard particles on the direction of crack propagation. Figure 8 (a) shows that the crack propagates straight to the particle located at 0° to the crack propagation direction. Figure 8(b) shows that the crack propagation direction can be changed toward a particle located at 10° to the current crack propagation direction. However, when the distance between a particle and a crack is greater than 3

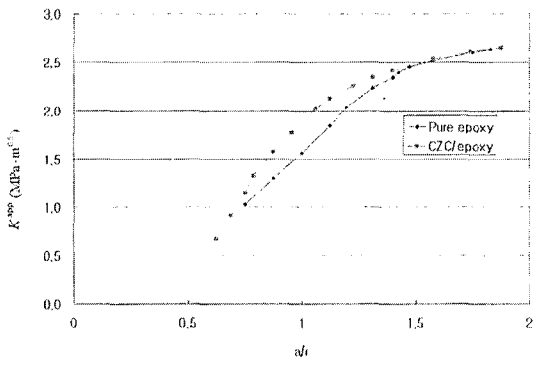

Fig. 7 Applied stress intensity factor against to the crack length over the radius of the hole (a/r). Under the displacement control of 1 mm/s, the stress intensity factor of CZC/epoxy composite was bigger than that of pure epoxy

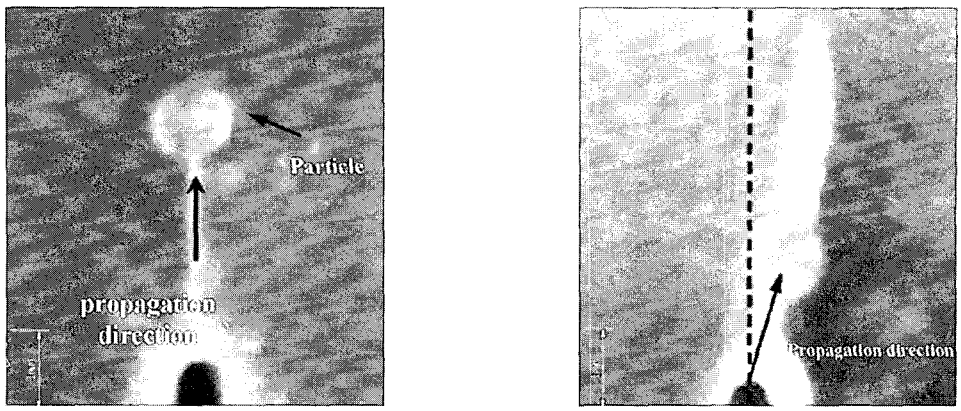

(a) (b)

Fig. 8 The effect of the location of a particle on the crack propagation direction. The specimens were tested in two forms ; one is that the particle was located on the same direction of precrack's propagation and the other is that the particle was 10° oblique. (a) shows that the crack propagates straight to the particle located at 0° to the crack propagation direction. (b) shows that the crack propagation direction can be changed toward a particle located at 10° to the current crack propagation direction.

mm, crack propagation maintained its current propagation direction regardless of the presence of a particle.

4. Discussions

The finite element analysis predicted that the crack propagation rates of the double cleavage drilled compression (DCDC) specimens will be over 4 times slower than those of double cleavage drilled tension (DCDT) specimens. Critchton and Tomozawa explained the crack propagation mechanism in DCDC specimens (Crichton and Tomozawa, 1999). Briefly, when a DCDC specimen is loaded in compression, the top and bottom of the hole in the specimen experience tensile stress, which at a certain load leads to the formation and growth of a pair of opposing cracks. The stress intensity decreases as the crack tips move farther away from the hole, and thus the crack growth rate decelerates as the crack grows under constant compression (Janssen, 1974). Due to this decreasing stress intensity after crack initiation, the DCDC test has a highly stress intensity-dependent crack velocity (Crichton and Tomozawa, 1999). From the above, it can be postulated that the differences between the crack propagation velocities of DCDC and DCDT specimens will increase as the crack grows. The ratio of the initial crack propagation speed in a DCDT specimen to that in a DCDC specimen will be a minimum because the stress intensity of the DCDC specimen will decrease as the crack tips move farther away from the hole. In Fig. 5, full-thickness crack initiation under $\dot{\sigma}_{app}=1$ N/mm^2/s occurred at 39 s for DCDC (double cleavage drilled compression) specimens but 9 s for DCDT (double compression drilled tension) specimens. Therefore, it is expected that the DCDC specimens will start its crack propagation at least 4.3 fold slower than the DCDT specimen.

In the present study, DCDC specimens were used to provide slower crack propagation speeds, which allowed in-situ direct observation of the crack propagation process. It took about 100 s for cracks to propagate by 3.5 mm under a displacement control of 0.01 mm/s. The average crack propagation speed ($\dot{a}$) for a crack less than 3.5 mm length was calculated as 0.034 mm/s. The crack velocities of DCDC specimens were reported to be successfully controlled in the range of $10^{-5}\sim10^{-1}$mm/s for various glass materials, only if specimens larger than $4\times4\times4$ mm^3 had been used (Crichton and Tomozawa, 1999 ; Lee and Tomozawa, 1999 ; Yoshida et al., 2001).

This DCDC specimen technique is considered

to be useful for in-situ observation of self-healing process polymer composite because self-healing process is important in micro scale. Nowadays, through an autonomic polymerization system incorporating a microencapsulated agent and catalyst, self-healing composites have emerged as interesting structural materials that can automatically cure fracture sites. Fracture test using DCDC specimens will usefully reveal self-healing processes in self-healing composites. A novel approach for the recovery of the fracture of thermosetting polymers has been introduced by White et al.(2001), and microcapsules facilitating in situ polymerization were developed to meet the requirements for a self-healing epoxy (Brown et al., 2003). Self-healing process is the propagating crack's interaction with agent and catalyst encapsulated by a capsule of nano-size thickness. The self-healing process triggered by microcapsules is performed sequentially, i.e., crack arrival at a microcapsule, microcapsule rupture, followed by the flow of healing agent into the crack (White et al., 2001). The sizes of these microcapsules fall in the range $50\times10^{-3}\sim500\times10^{-3}$ mm, and thus, it is difficult to observe the self-healing process with a conventional DCB or Chevron notch specimen.

Previous fracture studies of self-healing materials were not performed in-situ, i.e., the fracture plane of self-healing specimens was inspected after it was separated from fracture testing setup (Brown et al., 2002; 2004; Kessler and White, 2001; Kessler et al., 2003). Moreover, tensile loads were applied to double cantilever beam (DCB) specimens (Kessler and White, 2001), tapered double-cantilever beam (TDBC) specimens (Brown et al., 2002; 2004), or width tapered double-cantilever beam specimens (Kessler et al., 2003). To observe the in-situ healing process, crack propagation should be low to give sufficient time for the healing agent and catalyst to gel. The size of self-healing microcapsule is $10\times10^{-3}\sim1000\times10^{-3}$ mm (Brown et al., 2003). In the self-healing polymer composite, significant healing efficiency develops within 26 min, and this development time closely corresponds to the gelation time of the polyDCPD. If we set an assumption that gelation should be finished before the crack pass through a self-healing microcapsule then gelation should be finished in 26 min (= 1560 s) as a crack passes through a microcapsule. With the assumption, the required crack propagation speed to complete the gelation within 26 min would be $6.4\times10^{-5}\sim6.4\times10^{-4}$ mm/s for self-healing microparticles of $10\times10^{-3}\sim1000\times10^{-3}$ mm. Our DCDC fracture test showed a crack propagation velocity of 0.031 mm/s, but it can be still controlled to a much slower velocity by using a constant compression load control. In fact, other studies have shown DCDC glass specimen crack velocities in the range $10^{-5}\sim10^{-1}$ mm/s by using the constant load condition (Crichton and Tomozawa, 1999; Lee and Tomozawa, 1999; Yoshida et al., 2001). Although these studies were done using glass material and not a self-healing composite, the DCDC fracture testing achieved crack velocities of sub-micrometers per second under displacement control. Of course, if the gelation time is shortened by advances in the self-healing technique, the in-situ observation of the healing process could easily be achieved with the use of DCDC specimens.

Current study has several limitations. First, the analysis model for the finite element analysis (FEA) did not include the particles. Depending on the geometrical and mechanical features of particles, the crack propagation will show different fracture characteristics. However, the goal of the finite element analysis was to evaluate the crack propagation retardation function of the double cleavage drilled compression (DCDC) specimen compared to the double cleavage drilled tension (DCDT) specimen (Crichton and Tomozawa, 1999). Comparative fracture properties of DCDC and DCDT models will not be dependent on the presence of particles. Second, our experimental specimens included hard ceramic particles, which are not used in self-healing polymer composite. A crack passes through into a soft particle while it can not into a hard particle (White et al., 2001). Only soft micro-particles enable the tear of capsules and the flow of healing agent into cracked space. So, our experiment assessed only the crack retardation function of DCDC specimen tech-

nique for in-situ direct observation of the particle reinforced composite.

5. Conclusions

In the present study, we evaluated the feasibility of DCDC specimens to provide low crack velocities of 0.03 mm/s under 0.01 mm/s of displacement control. In addition, our finite element study confirmed the very low crack propagation rates of DCDC specimens. Using a transparent particle reinforced polymer composite and DCDC specimens, we were able to directly observe the crack propagation process. This study and literatures confirmed that DCDC specimens may introduce slow crack growth and eventually enable in-situ direct observation of retarded fracture process in particle composites such as the self-healing composite.

Acknowledgments

The authors gratefully acknowledge that this study was supported from the New University for Regional Innovation (NURI) Program prepared by the Korean Ministry of Education & Human Resources Development, and the Postdoctoral Fellowship Program of Korea Science & Engineering Foundation (KOSEF).

References

Brown, E. N., Sottos, N. R. and White, S. R., 2002, "Fracture Testing of a Self-healing Polymer Composite," *Experimental Mechanics*, Vol. 42, No. 4, pp. 372～379.

Brown, E. N., Kessler, M. R., Sottos, N. R. and White, S. R., 2003, "In Situ Poly (Urea-formaldehyde) Microcapsulation of Dicyclopentadiene," *Journal of Microcapsulation*, Vol. 20, No. 6, pp. 719～730.

Brown, E. N., White, S. R. and Sottos, N. R., 2004, "Mircocapsule Induced Toughening in a Self-healing Polymer Composite," *Journal of Materilals Science*, Vol. 39, pp. 1703～1710.

Crichton Stephen N. and Tomozawa Minoru, 1999, "Subcritical Crack Growth in a Phosphate Laser Glass," *Journal of the American Ceramic Society*, Vol. 82, No. 11, pp. 3097～3104.

He, H. Y., Turner, M. R. and Evans, A. G., 1995, "Analysis of the Double Cleavage Drilled Compression Specimen for Interface Frafcture Energy Masurements Over a Range of Mode Mixties," *Acta Metall. Mater*, Vol. 43, No. 9, pp. 3453～3458.

Janssen, C., 1974, "Specimen for Fracture Mechanics Studies on Glass," *Proceedings of the 10th International Conference on Glass*, Kyoto, Japan, Julu 8-13, pp. 10.23～10.30.

Janssen, C., 1980, "Fracture Characteristics of the DCDC Specimen, Report No. R-8074," *Corning Glass Works*, Corning, NY.

Jenne Thomas A., Keat William D. and Larson Michael C., 2003, "Limits of Crack Stability in the Double Cleavage Drilled Compression Specimen," *Engineering Fracture Mechanics*, Vol. 70, pp. 1697～1719.

Kagawa Yutaka and Goto Ken, 1998, "Direct Observation and Modeling of the Crack-fibre Interaction Process in Continuous Fibre-reinforced Ceramics : Model Experiments," Materials Science and Engineering, A250, pp. 285～290.

Kessler, M. R. and White, S. R., 2001, "Self-activated Healing of Delamination Damage in Woven Composites," Composites : Part A, Vol. 32, pp. 683～699.

Kessler, M. R., Sottos N. R. and White S. R., 2003, "Self-healing Structural Composite Materials," *Composites*, Part A, Vol. 34, pp. 743～753.

Lee, Y. K. and Tomozawa, M., 1999, "Effects of Water Content in Phosphate Glasses on Slow Crack Growth Rate," Non-crystalline Solids Vol. 248, pp. 203～210.

Michalske, T. A., Smith, W. L. and Chen, E. P., 1993, "Stress Intensity Calibration for the Double Cleavage Drilled Compression Specimen," *Engineering Fracture Mechanics*, Vol. 45, No. 5, pp. 637～642.

Weiderhorn, S. M., 1967, "Influence of Water Vapor on Crack Propagation in Soda-lime Glass," *Journal of the American Ceramic Society*, Vol. 50, No. 8, pp. 407～417.

White, S. R., Sottos, N. R., Geubelle, P. H., Moore, J. S., Kessler, M. R., Sriram, S. R., Brown,

E. N. and Viswanathan, S., 2001, "Autonomic Healing of Polymer Composites," Nature, Vol. 409, pp. 794~817.

Yoshida Satoshi, Jun Matsuoka and Naohiro Soga, 2001, "Crack Growth Behavior of Zinc Tellurite Glass With or Without Sodium Oxide," *Journal of Non-crystaline Solids*, Vol. 279, pp. 44~50.